THE JOURNAL OF BIOLOGICAL CHEMISTRY
Vol. 279, No. 8, Issue of February 20, pp. 6934–6942, 2004
Printed in U.S.A.

δ-Aminolevulinic Acid Dehydratase from *Plasmodium falciparum*

INDIGENOUS *VERSUS* IMPORTED*

Received for publication, October 17, 2003, and in revised form, November 13, 2003
Published, JBC Papers in Press, November 24, 2003, DOI 10.1074/jbc.M311409200

Shanmugham Dhanasekaran‡, Nagasuma R. Chandra§, B. K. Chandrasekhar Sagar¶, Pundi N. Rangarajan‡, and Govindarajan Padmanaban‡‖

From the ‡Department of Biochemistry, §Bioinformatics Centre and Interactive Graphics Facility, Indian Institute of Science, Bangalore 560012, India and the ¶Department of Neuropathology, National Institute of Mental Health and Neurosciences, Bangalore 560029, Karnataka, India

The heme biosynthetic pathway of the malaria parasite is a drug target and the import of host δ-aminolevulinate dehydratase (ALAD), the second enzyme of the pathway, from the red cell cytoplasm by the intra erythrocytic malaria parasite has been demonstrated earlier in this laboratory. In this study, ALAD encoded by the *Plasmodium falciparum* genome (PfALAD) has been cloned, the protein overexpressed in *Escherichia coli*, and then characterized. The mature recombinant enzyme (rPfALAD) is enzymatically active and behaves as an octamer with a subunit M_r of 46,000. The enzyme has an alkaline pH optimum of 8.0 to 9.0. rPfALAD does not require any metal ion for activity, although it is stimulated by 20–30% upon addition of Mg^{2+}. The enzyme is inhibited by Zn^{2+} and succinylacetone. The presence of PfALAD in *P. falciparum* can be demonstrated by Western blot analysis and immunoelectron microscopy. The enzyme has been localized to the apicoplast of the malaria parasite. Homology modeling studies reveal that PfALAD is very similar to the enzyme species from *Pseudomonas aeruginosa*, but manifests features that are unique and different from plant ALADs as well as from those of the bacterium. It is concluded that PfALAD, while resembling plant ALADs in terms of its alkaline pH optimum and apicoplast localization, differs in its Mg^{2+} independence for catalytic activity or octamer stabilization. Expression levels of PfALAD in *P. falciparum*, based on Western blot analysis, immunoelectron microscopy, and EDTA-resistant enzyme activity assay reveals that it may account for about 10% of the total ALAD activity in the parasite, the rest being accounted for by the host enzyme imported by the parasite. It is proposed that the role of PfALAD may be confined to heme synthesis in the apicoplast that may not account for the total *de novo* heme biosynthesis in the parasite.

Studies in this laboratory had demonstrated that the malaria parasites (*Plasmodium falciparum* and *Plasmodium berghei*) are capable of heme biosynthesis *de novo*, despite acquiring large amounts of heme from the host red cell hemoglobin in the intraerythrocytic stage (1, 2). Inhibition of the *de novo* heme biosynthetic pathway leads to death of the parasite and the pathway is therefore a drug target (1–3). Studies on the enzymes of the heme-biosynthetic pathway have revealed that the first enzyme, δ-aminolevulinate synthase, is coded for by the parasite genome and is localized in the parasite mitochondrion (4, 5). Studies from this laboratory have shown that the second enzyme of the pathway, δ-aminolevulinate dehydratase (ALAD),[1] in the parasite is of host origin and evidence was provided to show that the enzyme is translocated (imported) from the host red cell into the parasite and is functional (2, 3).

At the same time genome sequence data available for *P. falciparum* indicates that the parasite genome codes for ALAD (PfALAD) and other enzymes of the heme-biosynthetic pathway. Sato *et al.* (6) have shown by phylogenetic amino acid sequence analysis derived from truncated cDNA, including the metal-cofactor binding region and the active site, that PfALAD is more closely related to the Mg^{2+}-binding enzyme species from plant and algal plastids than the Zn^{2+}-binding species from animals and fungi. Subsequently, Sato and Wilson (7) have shown that the full-length PfALAD cDNA can complement a hemB mutant ($ALAD^{-/-}$) of *Escherichia coli*, indicating that the cDNA codes for a functional enzyme. These workers have also predicted the following. 1) PfALAD probably requires Mg^{2+} as a cofactor, although the metal ion may not serve as an allosteric activator. 2) It is possible that the intrinsic PfALAD is responsible for *de novo* heme synthesis in the parasite rather than the imported host enzyme.

It is therefore of interest to study the PfALAD in detail experimentally. In the present study, parasite gene-coded PfALAD-cDNA has been cloned and expressed in *E. coli*. The properties of the purified recombinant enzyme have been studied in detail, especially its metal ion requirement for activity. The enzyme has been modeled to explain some of its unique properties. It has been possible to raise antibodies that specifically interact with PfALAD and with these antibodies the localization of the enzyme in *P. falciparum* in culture has been studied by Western blot analysis and immunoelectron microscopy. Finally, based on studies on catalytic activity, inhibitor sensitivity, and localization of PfALAD, an assessment of the contribution of PfALAD to the total ALAD activity of the parasite in relation to the contribution of the imported host enzyme has been made.

* This work was supported in part by a grant from the Department of Biotechnology, New Delhi. The costs of publication of this article were defrayed in part by the payment of page charges. This article must therefore be hereby marked "*advertisement*" in accordance with 18 U.S.C. Section 1734 solely to indicate this fact.

‖ To whom correspondence should be addressed: Dept. of Biochemistry, Indian Institute of Science, Bangalore 560-012, India. Tel./Fax: 91-80-3601492; E-mail: geepee@biochem.iisc.ernet.in.

[1] The abbreviations used are: ALAD, δ-aminolevulinate dehydratase; ALA, δ-aminolevulinate; rmALAD, recombinant mouse ALAD; rPfALAD, recombinant *Plasmodium falciparum* ALAD; rPfΔALAD, truncated recombinant *Plasmodium falciparum* ALAD; PsALAD, *Pseudomonas aeruginosa* ALAD; hALAD, human erythrocyte ALAD; GST, glutathione *S*-transferase; aa, amino acid(s); PIPES, 1,4-piperazinediethanesulfonic acid; PBG, porphobilinogen.

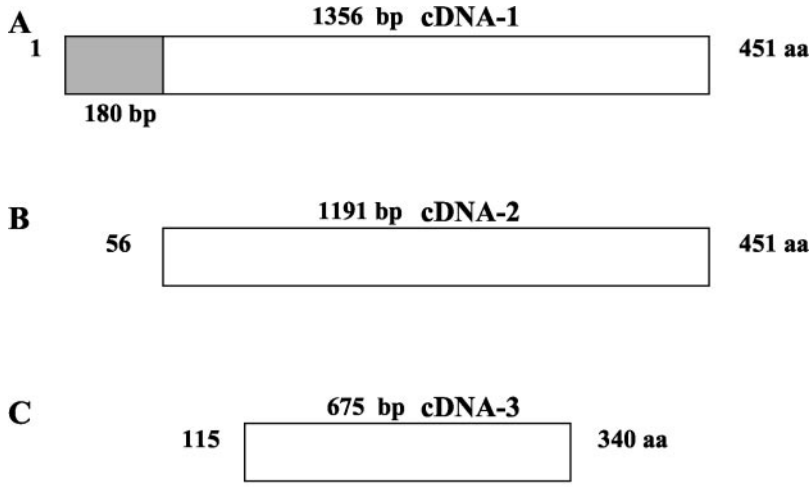

FIG. 1. **Scheme for ALAD, cDNA amplification.** Three different cDNAs were made using reverse transcriptase-PCR amplification of RNA isolated from *P. falciparum*. The length of cDNA products in nucleotide and amino acid (*aa*) coverage is indicated. The *stippled portion* in *A* indicates the postulated region encompassing the signal and transit peptide sequences.

EXPERIMENTAL PROCEDURES

Materials—Full-length mouse erythroid ALAD-cDNA clone was a kind gift from Dr. Terry Bishop, Johns Hopkins University, Baltimore, MD. Anti-mouse and anti-rabbit secondary antibodies were purchased from Invitrogen (ALP conjugates) or Pelco International (gold conjugates). All other chemicals were obtained from either Sigma or Invitrogen.

Parasite Maintenance and Isolation—P. falciparum culture was maintained on human O^+ red blood cells by the candle jar method (8). The cells were pelleted down and the parasites, essentially at the trophozoite stage, were isolated by treatment with 0.15% (w/v) saponin (9) or osmotic lysis (10) with slight modifications. For the latter procedure, packed infected erythrocytes were treated with 40 volumes of cold 10 mM potassium phosphate buffer, pH 7.4, mixed thoroughly and allowed to stand on ice for 10 min. The released parasites following lysis of the red cells were pelleted down and washed once again with the same buffer. The parasite pellet was subsequently washed three times with phosphate-buffered saline. With both procedures, the final washes were tested for possible hemoglobin or erythroid ALAD presence and were found to be undetectable.

Cloning of PfALAD cDNA—The full-length cDNA (cDNA-1) sequence of PfALAD was obtained from the genome data base and the sequence provided by Sato and Wilson (7). Reverse transcriptase-PCR amplification was carried out using the primer pair, PfALAD-1 (5′-ATGTTAAAATCAGATGTAGTGC-3′) and PfALAD-5 (5′-TCATAGAGTTAATTCAATATTTAAA-3′) to give a 1356-bp fragment (1–451 amino acids). A second cDNA (cDNA-2) was obtained using the primer pair, PfALAD-2 (5′-AATTCACAAATATTAAGTAAAATGAA-3′) and PfALAD-5 to give a 1191-bp fragment (56–451 amino acids). A third cDNA (cDNA-3) was obtained using the primer pair PfALAD-3 (5′-CACAAATATAAAGACATCGAAACTT-3′) and PfALAD-4 (5′-TCATCCCCCTCTATAATATGTTTATCCA-3′) to give a 675-bp product (115–340 amino acids) (Fig. 1, *A–C*). Because the primers were designed with EcoRI/BamHI linkers, all cDNAs (cDNA-1, -2, and -3) were cloned into pRSET vectors (Invitrogen, CA) at the BamHI-EcoRI site and proteins were expressed in *E. coli* BL21(DE3) after isopropyl-1-thio-β-D-galactopyranoside induction. Whereas the expression of cDNA-1 was very poor, cDNA-2 (56–451 aa) and cDNA-3 (115–340 aa) could be expressed in pRSET A vector. cDNA-2 was also cloned into PGEX4T1 vector to express the protein as GST fusion. In both cases, the *E. coli* cells were initially grown to an A_{600} of 1 at 30 °C with constant shaking at 200 rpm. The culture was then shifted to 18 °C and shaken at 150 rpm for 30 min before isopropyl-1-thio-β-D-galactopyranoside (0.5 mM) addition. Induction was carried out for 15 h. These conditions resulted in cDNA-2 being expressed in the soluble phase. In the case of His-tagged protein the frozen *E. coli* cells were lysed in lysis buffer (50 mM Tris buffer, pH 8.5) by sonication. The supernatant after centrifugation (20,000 rpm for 30 min) was subjected to ammonium sulfate fractionation (0–35%). The pellet was resuspended in 50 mM Tris, pH 8.5, containing 300 mM KCl and bound to nickel-agarose (Qiagen). After washing the column with equilibration buffer and the buffer containing 0.1% Triton X-100 (w/v) and 30 mM imidazole, the bound protein was eluted with a 30–300 mM imidazole gradient in the same buffer containing 0.1% Triton X-100. The peak fractions containing the protein were pooled, dialyzed against 50 mM Tris, pH 8.5, containing 20% glycerol, and stored at −20 °C.

In the case of the GST fusion protein, the recombinant *E. coli* lysate obtained with 50 mM Tris, pH 8.5, containing 0.5% Triton X-100 was centrifuged and the supernatant was directly loaded onto GST-agarose (Sigma) and washed with the same buffer containing 300 mM KCl. The protein was eluted with 50 mM Tris, pH 8.5, containing 30 mM GSH. The peak fractions were pooled and incubated with thrombin for 15 h at 4 °C to cleave the GST. The protein was purified on a Superdex-200 gel filtration column and equilibrated with 50 mM Tris, pH 8.5, containing 300 mM KCl using AKTA purifier (Amersham Biosciences). The fractions containing the enzyme were pooled and concentrated by ultrafiltration using a 50-kDa cut-off membrane (VivaScience). cDNA-3 (115–340 aa) was also expressed with histidine tag, but the protein was present in inclusion bodies. It was solubilized using 8 M urea and purified using the nickel-agarose column. The urea was dialyzed out after the protein was eluted from the column. cDNA-2 (56–451 aa) expressed with histidine tag or as a GST fusion protein (before and after removal of GST) was enzymatically active and was used as the source of the recombinant PfALAD (rPfALAD) in this study. The product of cDNA-3 (115–340 aa) expression is referred to as rPfΔALAD in this study and was used to obtain PfALAD-specific antibodies.

Native human ALAD was purified from human red blood cells by a slight modification of the known procedure (11). Briefly, the soluble red cell supernatant was subjected to DEAE-Sephacel chromatography, ammonium sulfate fractionation (0–45%), octyl-Sepharose and phenyl-Sepharose chromatography. The last two chromatography steps were repeated to obtain a pure preparation and this was used to raise antibodies to the host ALAD. Recombinant mouse ALAD (rmALAD) was purified as a protein with histidine tag from the clone (gift) and used to study the properties in comparison with rPfALAD. The mammalian enzyme species are highly conserved (12) and the properties of the mouse and human enzymes are very similar.

Enzyme Assay—ALAD enzyme activity was assayed in a total volume of 0.1 ml in a mixture containing 25 mM Trizma (Tris base) (to cover the pH range 7 to 9). Routine assays were carried out at pH 7.5 (25 mM PIPES) and 8.5 (25 mM Tris), in the presence of 5 mM ALA, 5 mM β-mercaptoethanol, and enzyme (0.5 to 2.0 μg of recombinant proteins or 150–200 μg of protein of parasite extract). The mixture was incubated at 37 °C for 1 h and the porphobilinogen (PBG) formed was estimated using modified Ehrlich reagent (13). No buffer ion effect as such on enzyme activity was seen. While studying the effects of EDTA or *o*-phenanthroline, the enzymes were first incubated with the chelator for 20–30 min before the addition of metal ions and ALA. A molar extinction coefficient for PBG of 60,200 M^{-1} cm^{-1} was used to quantitate PBG concentration. The specific activity of rmALAD ranged mostly between 22 and 26 μmol of PBG/mg of protein/h at pH 7.5. The corresponding values for rPfALAD ranged between 3 and 4 μmol of PBG/mg of protein/h at pH 8.5 and 2–2.5 μmol of PBG/mg of protein/h at pH 7.5.

Determination of Mg^{2+} Binding by Atomic Absorption—Metal ion stoichiometry was determined by atomic absorption using a Thermo Jarrell Ash Video 11E aa/ae spectrometer. Purified rPfALAD (5 ml, 400 μg of protein/ml), isolated with a histidine tag, was dialyzed against 500 ml of Tris buffer (100 mM, pH 8.5) containing 20% glycerol with three changes at 4-h intervals. The enzymatically active preparation was used to measure the intrinsic Mg^{2+} content.

PfALAD Homology Modeling—Alignment of the sequence (accession

number CAC82990/Q8MYK5) of PfALAD with the sequence neighbors identified by a BLAST (14) search of the Non-Redundant and Protein Data Bank (15) data bases, indicated ALAD from *P. aeruginosa* (PsALAD, Protein Data Bank codes 1B4K and 1GZG) (16, 17) to be the closest structural template with sequence similarities of 56% (*E* value: $3e^{-50}$) over 330 amino acid residues. The alignment with the template, when carefully verified by examining additional pairwise (18) and multiple alignments (19) with other closely related sequences, indicated a few local frameshifts as judged by the position of well conserved known functional residues, which were then corrected by minor editing. The model of the mature polypeptide of a subunit was built using Insight-II (Accelrys Inc.) using homology modeling protocols. The few insertions in the PfALAD were built using the distance matrix-based loop searching method available in Insight-II. The model was then soaked in a 5-Å layer of water molecules and energy was minimized initially using a steepest descent algorithm and then with a conjugate gradient minimizer. The octamer of PfALAD was built based on the octamer in PsALAD and the components were energy minimized individually as dimers and tetramers. PfALAD model was also compared with the structure of human erythrocyte ALAD (hALAD, Protein Data Bank code 1E51). Structural comparisons were carried out through a DALI (20) analysis. Various manipulations and analyses were carried out using Insight-II.

Localization of ALAD in P. falciparum—The parasite in culture was used to analyze for host and PfALAD by Western blot analysis and immunoelectron microscopy. For Western blot analysis, purified rPfALAD, partially purified native human ALAD, as well as parasite extracts were subjected to 10% SDS-PAGE and then transferred to nitrocellulose membranes for immunoblot analysis. Duplicate blots were screened with antibodies to the human red cell enzyme and rPfΔALAD with antibody dilutions in the range of 1:1000 to 1:2000 followed by goat anti-rabbit (human ALAD) or goat anti-mouse (rPfΔALAD) antibodies conjugated to alkaline phosphatase.

For immunoelectron microscopic studies, the parasite-infected red blood cell pellet was washed three times with phosphate-buffered saline and then resuspended in 1% (w/v) paraformaldehyde and 0.2% (w/v) glutaraldehyde in phosphate buffer, pH 7.1, for 3–4 h. Immunostaining was then carried out by the protocol supplied by PELCO International using the LR White resin. Ultrathin sections from the embedded block were mounted on nickel grids. All incubations with antibodies were carried out in blocking buffers containing 2% (w/v) bovine serum albumin. Anti-human ALAD antibodies (rabbit) or anti-rPfΔALAD antibodies (mouse) were used at 1:200 dilution and incubated for 2–3 h. Goat anti-rabbit or goat anti-mouse IgG coupled to 10- or 20-nm gold particles were used as secondary antibodies at 1:50 dilution and incubated for 1 h. The grids were then post-fixed with 1% glutaraldehyde in phosphate-buffered saline, washed with distilled water, subjected to silver enhancement, and then counterstained with uranyl acetate in 50% (w/v) ethanol. Sections were viewed using a JOEL CX100 transmission electron microscope.

Other Procedures—RNA was isolated from the parasite using Trizol (Invitrogen, CA). Antibodies were raised to purified native human ALAD in rabbits and to rPfΔALAD in mice. The parasite lysate was prepared by resuspending the parasite pellet in 50 mM Tris, pH 8, followed by freeze-thawing and sonication. The sonicate was then incubated with 0.5% Triton X-100 for 30 min in ice to obtain the total ALAD activity in the soluble phase. Partially purified hALAD and rPfALAD were used as controls. The assays were done in the presence or absence of 25 mM EDTA. Human red blood cell lysate was fractionated on a DEAE column to remove hemoglobin and partially purify hALAD.

RESULTS

The full-length cDNA (cDNA-1) for PfALAD was cloned into *E. coli* but the expression was very poor. This could be because of the hydrophobic signal sequence at the N terminus. Therefore cDNA-2 (56 to 451 aa) that permitted good growth of the *E. coli* hemB mutant in the complementation assay (7) was cloned into *E. coli* and expressed as a protein with the histidine tag or as a GST fusion protein (Fig. 2, *A* and *B*). Application of PlasmoAP (21), a rule-based predictor for apicoplast targeting peptides within *P. falciparum*, revealed that the N-terminal 70 amino acids would encompass the signal and transit peptides necessary to target ALAD to the apicoplast. Therefore, the removal of the N-terminal stretch (1–55 amino acids) should not affect enzyme activity. All the purified rPfALAD preparations, with histidine tag and with or without GST, were enzymatically active. Because, the histidine-tagged protein yields were higher than the GST-cleaved preparation, the former was used in most of the experiments. The purified rPfΔALAD (Fig. 2*C*) was used to raise PfALAD-specific antibodies.

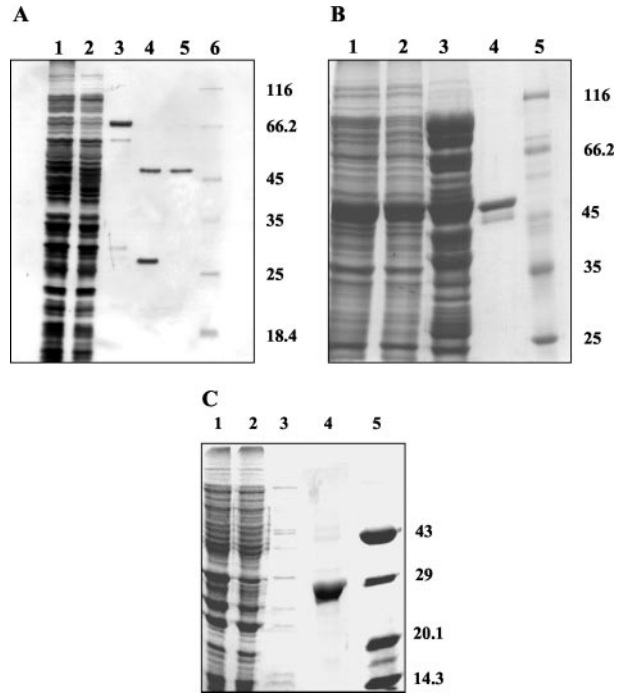

FIG. 2. **Expression of rPfALAD as GST fusion protein or with histidine tag.** The 1191- (cDNA-2) and 678-bp (cDNA-3) products were cloned into pGEX4T1 or pRSET vectors and the proteins were expressed with isopropyl-1-thio-β-D-galactopyranoside in *E. coli* BL21(DE3) as described in the text. *A*, purification profile of rPfALAD as a GST fusion protein. Lanes: *1*, *E. coli* lysate supernatant; *2*, flow through from a glutathione-agarose column; *3*, eluate from the column with reduced glutathione; *4*, preparation after thrombin cleavage; *5*, rPfALAD after gel filtration; *6*, molecular weight markers. *B*, purification profile of rPfALAD with the histidine tag. Lanes: *1*, *E. coli* cell lysate; *2*, soluble supernatant; *3*, 0–30% $(NH_4)_2SO_4$ fraction; *4*, eluate from the nickel-agarose column with imidazole; *5*, molecular weight markers. *C*, purification profile of rPfΔALAD with the histidine tag. Lanes: *1*, *E. coli* lysate; *2*, 8 M urea soluble fraction; *3*, flow through from the nickel-agarose column; *4*, eluate from the nickel-agarose column with imidazole; *5*, molecular weight markers.

Oligomeric Nature

Because most ALADs purified so far are octamers (22, 23), an assessment of the oligomeric state of rPfALAD was made based on the gel filtration profile on a Superdex 200 analytical FPLC column. The results presented in Fig. 3*A* indicate that the rPfALAD elutes from the column with an M_r of 345,000 compared with the value of 335,000 obtained for rmALAD. The subunit M_r values for rPfALAD and rmALAD are 46,000 and 38,000 on the basis of mobility on SDS-PAGE (Fig. 3*B*). Thus, both ALAD species are octamers.

pH Optimum and K_m

Because ALADs from plant sources have an alkaline pH optimum (23), it was of interest to assess the same with rPfALAD. The results presented in Fig. 4 reveal that rPfALAD indeed has a pH optimum between 8 and 9, whereas rmALAD has a pH optimum between 7.5 and 8.5. The K_m value for ALA with rPfALAD is 0.208 mM at pH 8.5, whereas for rmALAD at pH 7.5 the value is 0.294 mM.

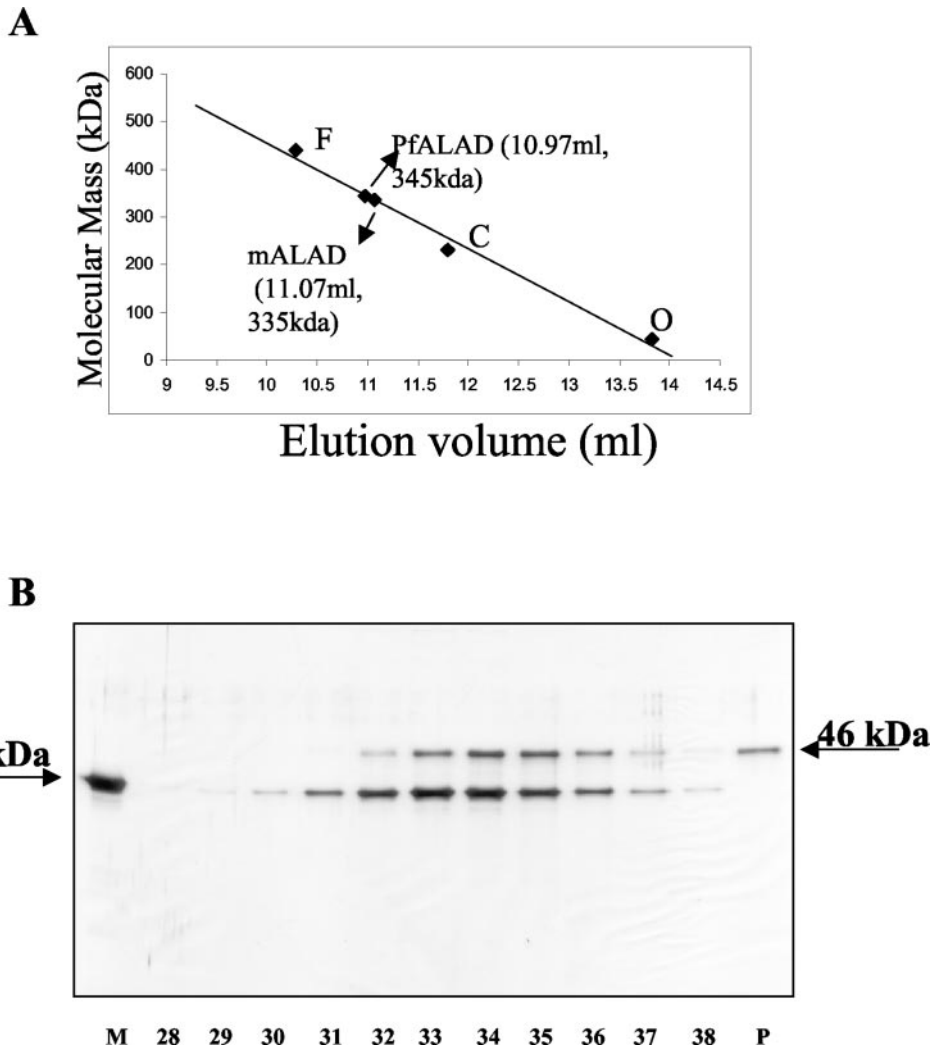

FIG. 3. **Elution profile of rmALAD and rPfALAD on Superdex-200 column.** The two preparations were mixed and loaded onto a Superdex-200 HR 10/30 (bed volume = ~24 ml) column, calibrated separately with ferritin (*F*), catalase (*C*), rmALAD (*A*), and ovalbumin (*O*). 200-μl fractions were collected and the fractions were subjected to 10% SDS-PAGE. *A*, elution profile of rmALAD and rPfALAD in relation to the molecular weight markers. *B*, SDS-PAGE analysis of the column fractions. Lanes: *M*, rmALAD marker. *P*, rPf ALAD maker. *28–38*, column fractions.

Effect of Metal Ions

A considerable amount of literature exists on the metal cofactor requirement of ALAD from different sources (22–27). The enzyme species are classified into five different types based on whether they require Zn^{2+} (mammalian and yeast), Mg^{2+} (plant, algae, and bacteria), or both (some bacteria). All the reported enzymes are inhibited by EDTA (26) or *o*-phenanthroline (24) and the inhibition can be overcome by the addition of Mg^{2+} or Zn^{2+}, depending on the enzyme species. Interesting results are obtained with rPfALAD in this regard. First of all, rPfALAD purified as described under "Experimental Procedures" and dialyzed extensively against 100 mM Tris buffer, pH 8.5, in the presence of 20% glycerol is active without addition of any metal ion. However, addition of Mg^{2+} stimulates enzyme activity by 20–30% at pH 8.5. As expected, the activity of rmALAD is not stimulated by Mg^{2+} (Fig. 5*A*). The unique features of rPfALAD are manifest in experiments studying the effects of EDTA and *o*-phenanthroline. EDTA does not inhibit rPfALAD enzyme activity even at 25 mM concentration and overnight treatment. Treatment of the enzyme with Chelex 100 resin does not lead to loss of enzyme activity (data not presented). RmALAD is inhibited to an extent of 90% at 5 mM EDTA concentration (Fig. 5*B*).

Whereas EDTA does not inhibit the basal activity of rPfALAD, it inhibits the stimulation brought about by added Mg^{2+}. *o*-Phenanthroline inhibits rmALAD activity by more than 90% at 0.5 mM concentration and this inhibition is substantially reversed in the presence of 20–40 μM Zn^{2+}. rPfALAD activity is inhibited to 70% by *o*-phenanthroline at 5–10 mM concentration and this inhibition is not reversed in the presence of 10–250 μM Zn^{2+}, either at pH 7.5 or 8.5. Interestingly, Mg^{2+} stimulation of rPfALAD is seen with the untreated or *o*-phenanthroline-treated enzyme. It is concluded that the inhibitory effects of *o*-phenanthroline on PfALAD are not related to removal of any metal ion such as zinc. In fact, Zn^{2+} as such is very inhibitory to rPfALAD activity. At pH 8.5, the enzyme activity is inhibited by 50% at 75 μM Zn^{2+}, and at pH 7.5 the metal is even more inhibitory, 50% inhibition being brought about by less than 20 μM Zn^{2+}. The 50% inhibitory value for rmALAD at pH 7.5 is around 120 μM Zn^{2+} (data not presented).

Effect of Monovalent Cation

rPfALAD activity is also stimulated by K^+ and this activation is pH-dependent. Between pH 6.5 and 7.0, K^+ is as stimulatory as Mg^{2+} and the stimulation is almost 2-fold. However, while the stimulatory effect of Mg^{2+} (around 20–30%) is seen

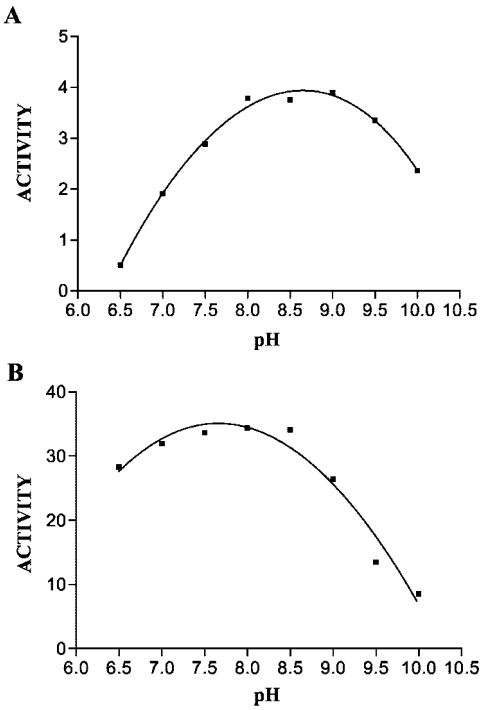

FIG. 4. **pH profiles for rmALAD and rPfALAD enzyme activities.** PIPES, Tris, and Trizma buffers were used to cover the pH range as indicated in the text. *A*, rPfALAD. *B*, rmALAD. The enzyme activity is expressed as μmol of PBG/mg of protein/h.

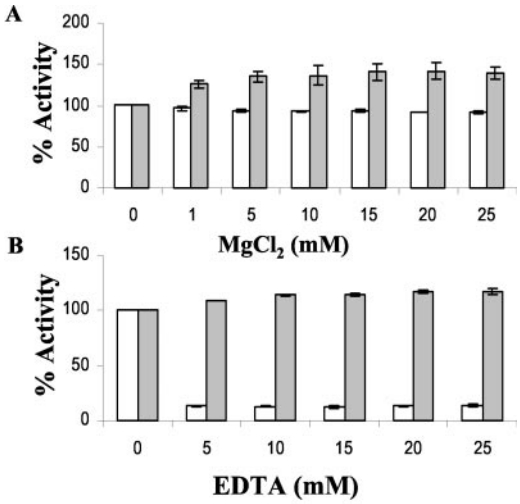

FIG. 5. **Effect of Mg^{2+} and EDTA on rmALAD and rPfALAD enzyme activities.** While rmALAD was assayed at pH 7.5, rPfALAD was assayed at pH 7.5 (data not presented) and 8.5. *A*, effect of Mg^{2+} on the two enzyme activities. *B*, effect of EDTA on the two enzyme activities. *Open bar*, rmALAD; *stippled bar*, rPfALAD. The activity of untreated enzyme (μmol of PBG formed per mg of protein/h) is taken as 100%.

at all pH values tested (6.5–10) the effect of K^+ wanes at pH values above 7 and is actually slightly inhibitory at pH 8.5 (Fig. 6). It thus appears that K^+ and Mg^{2+} act at different sites on the enzyme. Atomic absorption spectrometric analysis of purified, enzymatically active rPfALAD that was dialyzed extensively against 100 mM Tris buffer, pH 8.5, containing 20% glycerol reveals that the enzyme contains 2 atoms of Mg^{2+} per octamer of the enzyme.

Modeling of PfALAD Structure

ALAD asymmetrically condenses two molecules of ALA to produce PBG. The two ALA substrate molecules are distinguished as A- and P-site ALA because of the acetic acid and propionic acid side chains that they contribute to the product. The corresponding binding sites on ALAD are termed A-site and P-site, respectively. The sequence of PfALAD is structurally compatible with the TIM barrel-fold exhibited by all the other known structures of ALAD including the human enzyme (16, 28, 29). It also contains the additional strands and helices located in a long extended N-terminal arm, as seen in other ALAD structures. The structure-based alignment of the amino acid sequence of PfALAD with PsALAD was carried out as described under "Experimental Procedures" (Fig. 7*A*). A model of the octamer was constructed for PfALAD based on the arrangement seen in the PsALAD. Despite overall similarities in sequence, subunit, and quaternary structures between PfALAD and PsALAD, several fine differences exist. The sequence alignment of PfALAD with PsALAD reveals 3 single residue deletions and 6 short insertions spanning 1–4 residues distributed across the PfALAD primary structure. It is interesting to observe that 2 of the deletions and 3 of the insertions occur at the dimer-dimer interface such that the corresponding residues of the A subunit can interact with those of the E subunit. The insertion corresponding to residues 362–365 in PfALAD is an extended loop that projects toward the tetrameric axis stabilized by a salt-bridge formed by Lys^{363} and Asp^{365} present within the loop of each subunit. Because the octamer can be viewed as two tetramers stacking against each other, the extended loops of one tetramer stack against those of the other. Another insertion corresponding to residues 390–392 is at the interface of two subunits forming a dimer.

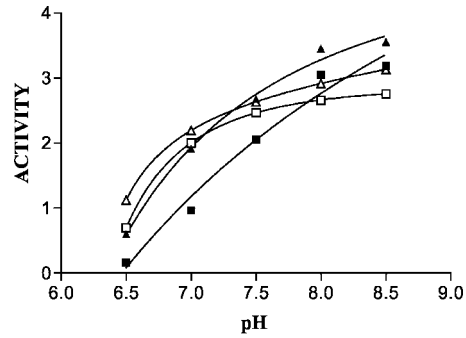

FIG. 6. **Effect of K^+ and Mg^{2+} on rPfALAD enzyme activity as a function of pH.** Effect of K^+ on enzyme activity in the presence of added Mg^{2+} as a function of pH. ■, no metal addition; □, 100 mM KCl; ▲, 10 mM $MgCl_2$; △, 100 mM KCl + 10 mM $MgCl_2$. The enzyme activity is expressed as μmol of PBG/mg of protein/h.

Substrate Binding Sites—The residues in both the A-site as well as in the P-site are essentially identical in both enzymes, suggesting a mode of binding for the substrates similar to that in PsALAD, and indeed in all the other ALAD structures known so far. A series of events leading to the formation of a fully assembled active site (monomer A in dimer AB) has been proposed for PsALAD (17). These are (*a*) entry of monovalent cation to the catalytic center that is then stabilized by Asp^{127}, Asp^{131}, and Ser^{175}, a water molecule, and the amino group of P-site ALA; (*b*) formation of Schiff base with the A-site ALA by Lys^{205}; (*c*) occupation of the C-site by Mg^{2+} disrupts the interaction between Asp^{139} and Arg^{181}. This allows Asp^{139} to flip into the active site to further stabilize the A-site ALA; and (*d*) formation of hydrogen bond between Asp^{139} and Lys^{229}, leading to the closure of the active site flap and formation of fully assembled, catalysis-ready active site.

However, the substrate binding site of PfALAD appears to be more integral because of several additional stabilizing factors especially in the environment of Lys^{316} (229 in PsALAD) whose proper orientation and interaction with the substrate are a

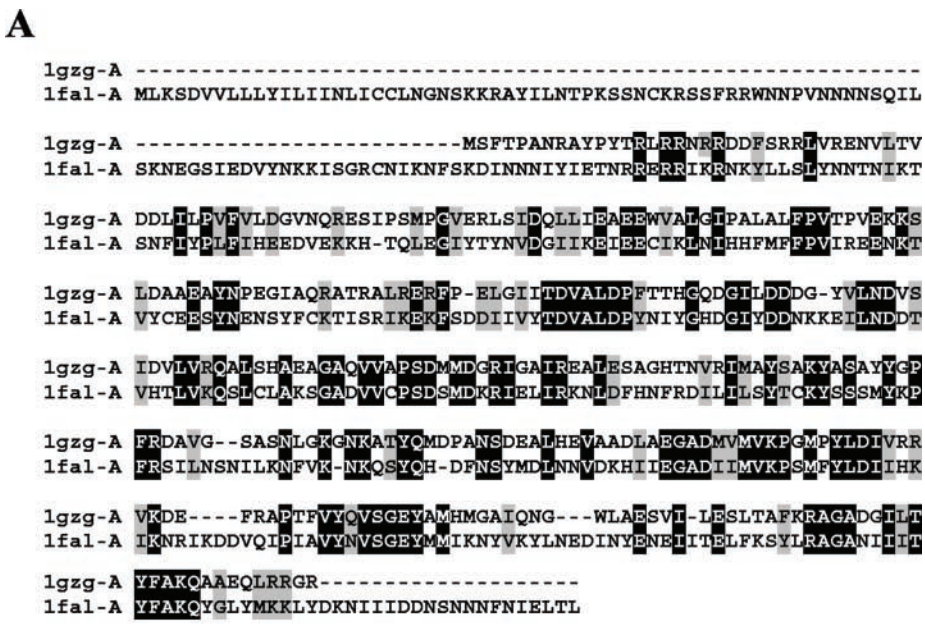

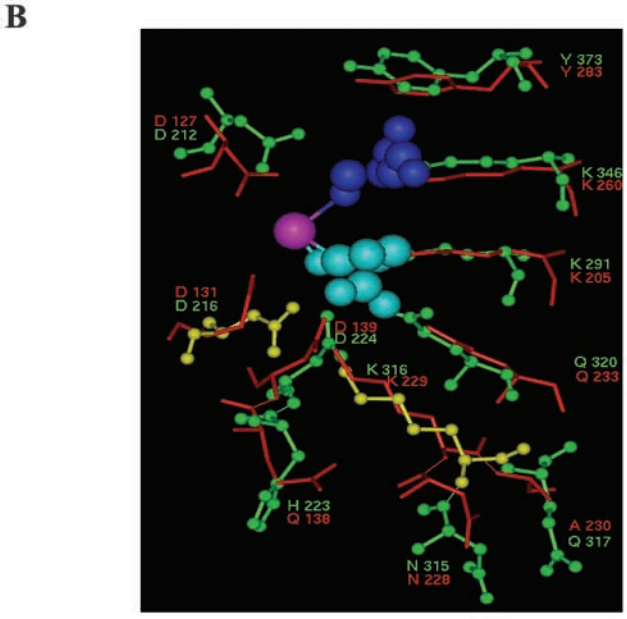

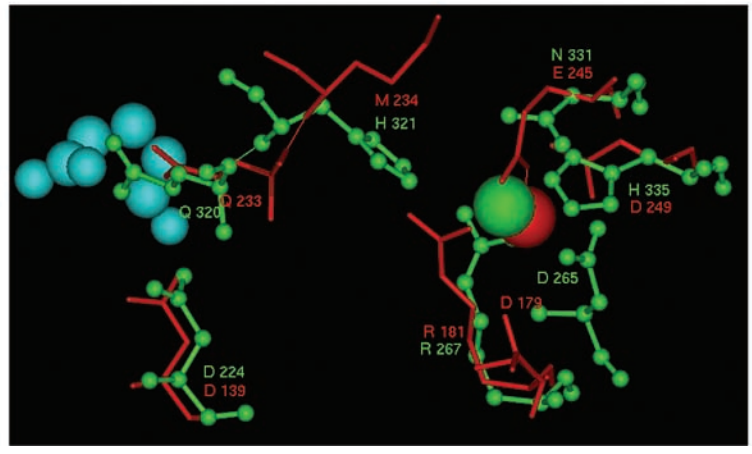

FIG. 7. **Modeling studies on PfALAD.** *A*, sequence based alignment of PfALAD and PsALAD. Identical residues are highlighted in *black*, whereas similar residues are highlighted in *gray*. *B*, a view of the active sites of PfALAD (*green/ball and stick*) and PsALAD (*red/stick*). The Cα atoms of the corresponding subunits have been superposed in the two structures (root mean square deviation 1.6). The A-site 5-fluorolevulinic acid is shown in *cyan*, the P-site 5-fluorolevulinic acid is shown in *blue*, and the Na^+ ion is shown in *pink* (CPK models). Lys^{316} and Asp^{216} of PfALAD are shown in *yellow* and their significance is discussed in the text. *C*, a view of the Mg^{2+}-binding C-site in monomer A of PfALAD and PsALAD. The coloring and representation are the same as that in Fig. 9*B*. Mg^{2+} (CPK model) docked into the C-site is also shown. Gln^{320} of PfALAD (Q233 in PsALAD) and A-site 5-fluorolevulinic acid are shown for reference. Asp^{224} and Arg^{267} of PfALAD differ in conformation from their corresponding residues Asp^{139} and Arg^{181} in PsALAD that form a salt bridge in monomer B (open form).

prerequisite for catalysis. These changes in PfALAD are (*a*) Asp^{216} (131 in PsALAD) is oriented appropriately to form a salt bridge with Lys^{316} replacing the Asp^{139}-Lys^{229} interaction in PsALAD. This can happen because the conformation of Asp^{216} is altered slightly because of the influence of an insertion at position 205 and a change in the amino acid sequence from position 218 to 221 in PfALAD; (*b*) the two adjacent residues, Asn^{315} and Gln^{317}, form bidentate hydrogen bonds in PfALAD that are absent in PsALAD; and (*c*) His^{223}, which is in the vicinity of Lys^{316}, keeps the Lys^{316} fixed and oriented (to avoid charge repulsion) toward the substrate. PsALAD lacks this histidine and has Gln^{138} in its place. Therefore, in PfALAD the positioning of the stretch from Lys^{316} to Gln^{320} seems to be prefixed because of the network of interactions highlighted (Fig. 7*B*).

C-site Magnesium and Its Communication with the Active Site—Glu^{245} in *P. aeruginosa* or its equivalent in plants is responsible for coordinating Mg^{2+} at the C-site. In PfALAD, Glu^{245} is replaced by Asn^{331} and this change has been attributed earlier to a possible absence of C-site Mg^{2+} binding in PfALAD (7). However, an enhancement of catalysis in the presence of added Mg^{2+} has been observed in the present study. Despite differences in amino acid residues at the C-site, energy minimization of the PfALAD model with magnesium docked into the site suggests that such a binding is energetically and geometrically feasible. In the PfALAD model, Asp^{265} (179 in PsALAD) is capable of coordinating Mg^{2+} through its carboxylate side chain and Asn^{331} is still positioned suitably for water-mediated coordination of the Mg^{2+} ion. In addition, His^{335} in PfALAD replacing an aspartic acid in PsALAD is also oriented appropriately for holding a Mg^{2+} ion. Although, metal ions have an overwhelming preference for carboxylates as their ligands in protein structures (30, 31), nitrogen donors such as in histidine imidazoles are also known to coordinate Mg^{2+} (32, 33). The other residues in the vicinity capable of coordinating Mg^{2+} through water molecules are Arg^{267} and His^{321} (Fig. 7*C*).

Because the parasite is importing the hALAD, it is of interest to compare the geometry of the PfALAD substrate binding site with that of hALAD. Significant differences were observed because hALAD requires Zn^{2+} for catalytic activity. The hALAD substrate binding site is stabilized by the presence of Zn^{2+}, which is coordinated by 3 cysteines. Asp^{216} and Asp^{224}, which help position Lys^{316} appropriately for catalysis in the PfALAD active site, are replaced by Cys^{124} and Cys^{132} in hALAD. The amino acid corresponding to PfALAD Lys^{316} is Arg^{221} in hALAD. In view of these differences, meaningful comparisons between active sites of PfALAD and hALAD cannot be made. The C-site metal binding pocket is absent in hALAD.

Sensitivity to Succinylacetone

This inhibitor is specific for ALAD, although different ALAD species manifest differential sensitivity (24, 34). The results presented in Fig. 8 reveal that rPfALAD and rmALAD are inhibited by succinylacetone, the latter being more sensitive than the former. Both enzymes are inhibited strikingly in the nanomolar range, 50% inhibition being brought about by 125 and 250 nM succinylacetone for rmALAD and rPfALAD, respectively. The host hALAD has also been partially purified and its succinyl acetone sensitivity is very similar to that of rmALAD.

Localization of ALAD in the Parasite

Studies were carried out to examine the localization of PfALAD in relation to that of the host enzyme in the parasite. Antibodies against the truncated protein rPfΔALAD react specifically with rPfALAD but not with the ALAD from human red blood cells in Western blot analysis. Antibodies to the human red blood cell ALAD are specific to the human enzyme (Fig. 9*A*). The results presented in Fig. 9*B* reveal that both the host ALAD and PfALAD are detected in the parasite lysate. Although the concentration of the host ALAD in the parasite is significantly higher than that of PfALAD, exact quantification is not possible, because the blot has to be developed much longer to obtain the weaker signal for PfALAD. These results are also corroborated by the immunoelectron microscopic analysis of the infected red cell. The data presented in Fig. 10, *A* and *B*, reveal that host ALAD is widely distributed in the parasite cytoplasm and food vacuole. PfALAD signal is sparse, although its presence in the apicoplast can be clearly seen Fig. 10, *C* and *D*. The distinctive four-membrane architecture that characterizes the apicoplast is reported to be fragile (35). This is the first report on the actual detection of an enzyme of the heme-biosynthetic pathway in the apicoplast.

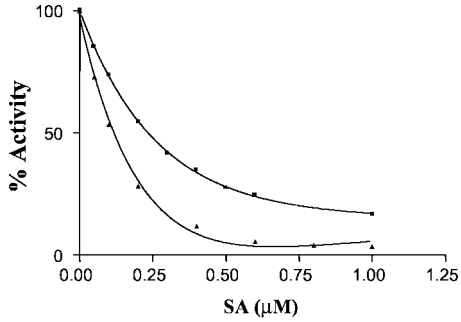

FIG. 8. **Inhibition of rPfALAD and rmALAD enzyme activities by succinylacetone (*SA*).** ■, rPfALAD; ▲, rmALAD. The enzymes were preincubated with succinylacetone for 20 min before the addition of 5 mM ALA. The activity of the untreated enzyme (μmol of PBG/mg of protein/h) is taken as 100%.

PfALAD and Host Enzyme Activity in the Parasite

It was of interest to assess the contribution of PfALAD to the total enzyme activity in the parasite, in view of the earlier reports from this laboratory on the import of the host enzyme into the parasite (2, 3). Having observed differential sensitivity of rPfALAD and rmALAD (as well as the native human red cell ALAD) to EDTA, the enzyme activities were assayed in the parasite lysate in the presence or absence of 25 mM EDTA. The results presented in Table I reveal that with total parasite extract the residual activity in the presence of EDTA is 13.8%, whereas the corresponding value for the host enzyme activity is 2.8%. Therefore, the contribution of PfALAD to the total ALAD activity in the parasite is around 11%.

DISCUSSION

The results obtained in the present study reveal that rPfALAD manifests properties expected of a plant-like enzyme species (alkaline pH optima and apicoplast localization), while at the same time manifesting certain unique properties such as Mg^{2+}-independent and EDTA-resistant catalytic activity. Interestingly, the enzyme from *P. aeruginosa* has also been shown not to require any divalent metal ion for activity. The bacterial enzyme has been shown to contain 4 atoms of Mg^{2+}, required for stabilizing the octameric structure but not essential for octamer formation or catalytic activity. This is the lowest number of bound, divalent metal ions yet reported for all species of ALAD except for rPfALAD, which is investigated in the present study. Hence, the enzyme from *P. aeruginosa* has been described as a novel type V ALAD (26, 36). rPfALAD resembles the enzyme from *P. aeruginosa* in most of its properties, except in terms of sensitivity to EDTA and dialysis. The dialyzed enzyme is active in the absence of added metal ions

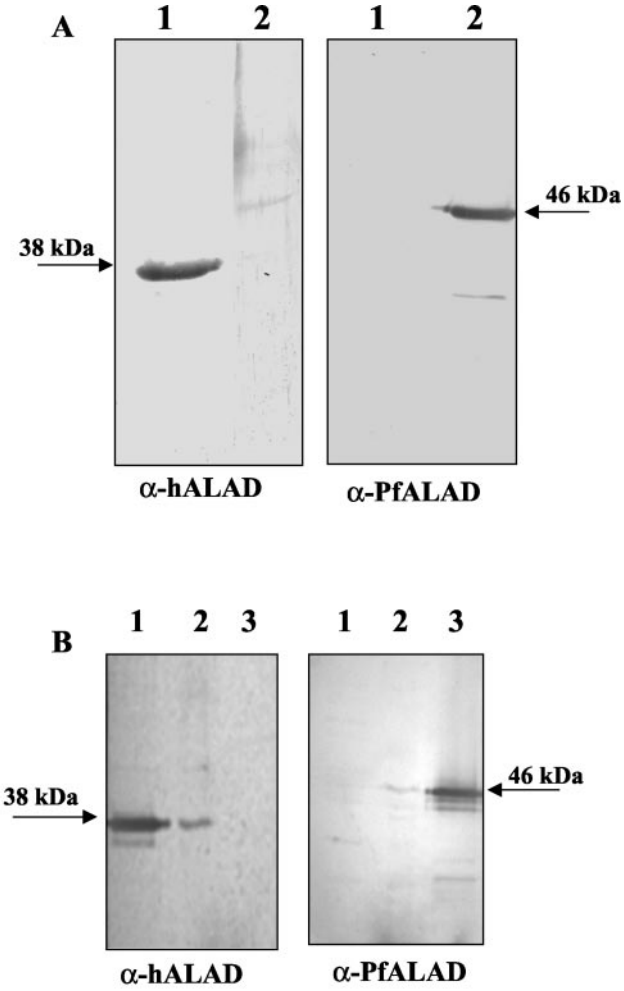

FIG. 9. **Localization of PfALAD in *P. falciparum* by Western blot analysis.** Antibodies to purified human erythroid ALAD (α-hALAD) and rPfΔALAD (α-PfALAD) were used in these experiments. Duplicate membrane blots were used for the analysis. *A*, antibody specificity. Lanes: *1*, human erythroid ALAD; *2*, rPfALAD. *B*, detection of host (human) and PfALAD in *P. falciparum*. Lanes: *1*, human erythroid ALAD; *2*, parasite lysate, *3*, rPfALAD.

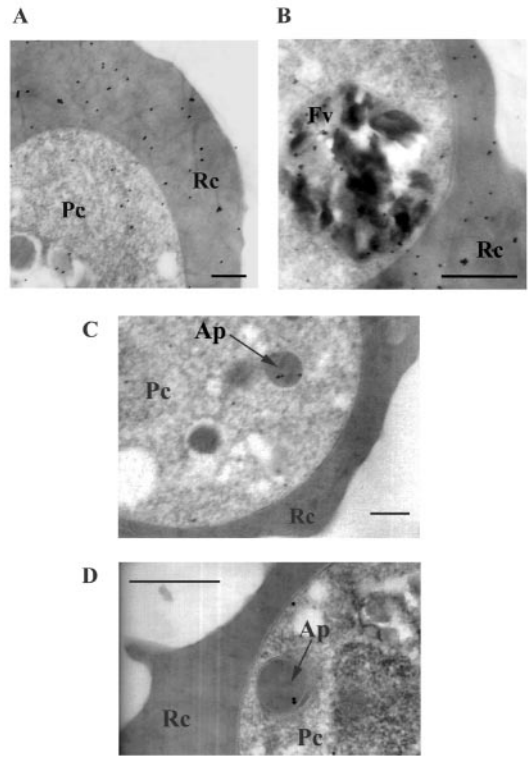

FIG. 10. **Localization of PfALAD in *P. falciparum* by immunoelectron microscopy.** *A* and *B*, localization of host ALAD in the parasite and red blood cell. *C* and *D*, localization of PfALAD in the apicoplast with multimembrane structure. The abundant presence of host ALAD in the cytoplasm and food vacuole and the sparse occurrence of PfALAD in the apicoplast (shown by the *arrow*) of *P. falciparum* is indicated by the distribution of gold particles. *Scale bar* = 0.5 μm. *Pc*, parasite cytoplasm. *Rc*, red cell cytoplasm. *Fv*, food vacuole. *Ap*, apicoplast.

but can be stimulated by the addition of Mg^{2+} to an extent of 20–30%. The dialyzed enzyme contains 2 atoms of bound Mg^{2+} per octamer, the significance of which is not clear at present. The Mg^{2+} dependence of plant and algal ALADs in chloroplasts has been explained because of the presence of a high concentration of Mg^{2+} (10 mM) that would help to overcome the thermodynamic difficulty of inserting Mg^{2+} into protoporphyrin IX for chlorophyll biosynthesis. This perhaps acted as the evolutionary pressure against a chlorophyll biosynthetic enzyme such as ALAD, to switch over to Mg^{2+} from Zn^{2+} as the metal requirement (37). Because, apicoplasts are held to be derived from algal plastids by secondary endosymbiosis (38), PfALAD perhaps shows Mg^{2+} dependence for activation. However, the concentration of Mg^{2+} in the apicoplast is not known.

The bacterial enzyme is completely inhibited by EDTA or just by dialysis and the apoenzyme can be reconstituted by Mg^{2+} (26, 36). The crystal structure of ALAD from *P. aeruginosa* reveals that Mg^{2+} is bound 14 Å away from the Schiff base-forming nitrogen atom of the active site lysine (16). Based on the crystal structure of the enzyme in complex with the inhibitor 5-fluorolevulinic acid at high resolution, the active site has been shown to contain a monovalent cation (Na^+) that may assist in enzyme activity (17). rPfALAD is similar to PsALAD in this regard and added K^+ stimulates the enzyme activity in the pH range between 6.5 and 7.5. However, as stated earlier, rPfALAD unlike PsALAD does not lose enzyme activity on dialysis and is active in the absence of added Mg^{2+} or K^+.

TABLE I
ALAD enzyme activity in P. falciparum extracts

Enzyme assay was carried out in the presence of 25 mM EDTA to distinguish between host ALAD (sensitive) and PfALAD (insensitive). Data given are representative of three independent experiments.

Fraction	ALAD activity	
	− EDTA	+ EDTA
	μmol PBG/mg protein/hr	*% residual activity*
Total activity[a] in parasite extract	0.011	13.8
Human red blood cell ALAD (DEAE fraction)	0.196	2.8
rPfALAD[b]	1.89	100

[a] Total activity represents activity obtained from the soluble and membrane-bound enzyme extracted as given under "Experimental Procedures."

[b] rPfALAD was assayed in the absence of metal ions.

Homology modeling studies were done to get insight into the unique properties of PfALAD discussed above. These studies have shown that the alterations in interactions arising out of the deletion and insertions in PfALAD, mentioned earlier, necessitate a minor reorientation of each subunit with respect to the others, as compared with that in PsALAD. In addition, there are a number of additional interactions between two dimers (*e.g.* A and E subunits of AB and EF dimers) in the PfALAD structure resulting in a stable octamer. The prefixed

nature of important active site amino acids (*e.g.* positioning of the stretch from Lys^{316} to Gln^{320}) might help to explain the observation that metal ions (either divalent or monovalent), which are normally required by other ALAD species to stabilize the hydrophilic network in the active site, are not required by PfALAD. Analysis of the PsALAD structure suggests that the conformation of the N-terminal arm of the B-subunit is dependent on the salt bridge made by Arg^{19} on this subunit with the A subunit Glu^{245}. This interaction is stabilized by magnesium binding to the C-site, which is at the interface of A and B subunits. In PfALAD, this interaction is absent but is compensated by other salt bridges between A/B and E subunits (B: Arg^{102}, Arg^{99}, Glu^{95} with E: Arg^{281}, Asp^{282}, and A: Lys^{232} with E: Asp^{256}) as well as by hydrophobic contacts between the B and E subunits (B: Leu^{109}, Ile^{103} with E: Leu^{284}, Ile^{208}). The Arg^{181}-Asp^{139} interaction proposed to form the communication between the C-site and active site in PsALAD may not exist in PfALAD although it cannot be totally ruled out. Instead, His^{321}, which is in the water-mediated coordination sphere of Mg^{2+} in PfALAD, is adjacent to Gln^{320} that directly interacts with the substrate in the A-site and hence can form a probable route of communication to the active site. Thus Mg^{2+}, although not required for catalytic activity or stabilization of the octameric structure in PfALAD, can bind to the C-site and stimulate the enzyme activity. X-ray crystal structural analysis of PfALAD would be of considerable interest.

Expression profiling using DNA microarray (39) reveals that PfALAD mRNA expression in the intraerythrocytic parasite is very low. The present studies reveal that the enzyme protein can be detected in low levels in the parasite by Western blot analysis, immunolocalization, and enzyme activity. Thus, the *Pfalad* gene is transcribed and translated. Sato and Wilson (7) have suggested that PfALAD may be responsible for parasite heme synthesis rather than the imported host enzyme. As a basis for this suggestion, these authors have drawn on the differential sensitivity between the pea *versus* yeast enzyme to succinylacetone (K_i = 0.3 μM *versus* 0.8 mM) (24), implying that the parasite enzyme is likely to resemble the pea enzyme. However, the present studies reveal that both rPfALAD, rmALAD and hALAD, are sensitive to succinylacetone in the nanomolar range, the host enzyme being more sensitive than the parasite enzyme to the inhibitor. However, the concentration of succinylacetone required to inhibit heme synthesis and growth in *P. falciparum* in culture exceeds 2 mM (1, 4) and it is obviously because of the abundance of the host ALAD in the red cell and the parasite. Thus, the argument for the involvement of PfALAD rather than that of the imported host enzyme in parasite heme synthesis, based on the presumed higher sensitivity of the parasite gene-coded enzyme than that of the host to succinylacetone is not tenable. Furthermore, earlier studies from this laboratory have shown that when *P. falciparum* is cultured in erythrocytes where the host ALAD is irreversibly inactivated by succinylacetone, the parasite ALAD levels fall dramatically leading to inhibition of heme synthesis and death of the parasite (2). Subsequent studies have shown that when a truncated polypeptide of host ALAD (ALAD-ΔNC) is added to a culture of *P. falciparum*, it is taken up by the parasite and it blocks the translocation of the host enzyme to the parasite cytosol, leading to inhibition of parasite heme synthesis and death of the parasite (3).

The real basis for the suggestion of Sato and Wilson (7) is the fact that *P. falciparum* has a functional *alad* gene. The present studies reveal that although the parasite has a functional *alad* gene, its contribution to the ALAD enzyme levels of the parasite is quantitatively small. This is borne out by a comparison between the imported host enzyme and the parasite genome-coded enzyme on the basis of Western blot analysis, signal abundance in immunoelectron microscopy, and assay of enzyme activity. It is clear that PfALAD contributes to around 10% of the total ALAD activity of the parasite. It appears possible that PfALAD may only take care of heme synthesis in the apicoplast and an additional site of heme synthesis involving the parasite mitochondrion and cytosol containing the imported host enzyme(s) is necessary for the synthesis of parasite hemoproteins. This mechanism is perhaps necessary, because there is only a single apicoplast in the parasite, unlike in plants where chloroplasts are present abundantly. The origin of ALA for apicoplast heme synthesis is still an open question.

Acknowledgement—We thank Dr. S. Subramanian, Indian Institute of Science, Bangalore, India, for help with the metal analysis of the proteins using the atomic absorption spectrometer.

REFERENCES

1. Surolia, N., and Padmanaban, G. (1992) *Biochem. Biophys. Res. Commun.* **187,** 744–750
2. Bonday, Z. Q., Taketani, S., Gupta, P. D., and Padmanaban, G. (1997) *J. Biol. Chem.* **272,** 21839–21846
3. Bonday, Z. Q., Dhanasekharan, S., Rangarajan, P. N., and Padmanaban, G. (2000) *Nat. Med.* **6,** 898–903
4. Wilson, C. M., Smith, A. B., and Baylon, R. V. (1996) *Mol. Biochem. Parasitol.* **75,** 271–276
5. Vardharajan, S., Dhanasekaran, S., Rangarajan, P. N., and Padmanaban, G. (2002) *Biochem. J.* **367,** 321–327
6. Sato, S., Tews, I., and Wilson, R. J. (2000) *Intl. J. Parasitol.* **30,** 427–439
7. Sato, S., and Wilson, R. J. (2002) *Curr. Genet.* **40,** 391–398
8. Trager, W., and Jensen, J. B. (1976) *Science* **193,** 673–675
9. Fitch, C. D., Chevli, R., Banyal, H., Phillips, G., Pfaller, M. A., and Krogstad, D. J. (1982) *Antimicrob. Agents Chemother.* **21,** 819–822
10. Sirawaraporn, W. (1985) in *Genetic Engineering Techniques in Tropical Diseases Research* (Panyim, S., Wilairat, P., and Yuthavong, Y., eds) pp. 407–412, Mahidol University, Bangakok
11. Anderson, P. M., and Desnik, R. J. (1979) *J. Biol. Chem.* **254,** 6924–6930
12. Jaffe, E. K. (2000) *Acta Crystallogr. Sect. D Biol. Crystallogr.* **56,** 115–128
13. Mauzerall, D., and Granick, S. (1956) *J. Biol. Chem.* **219,** 435–446
14. Altschul, S. F., Gish, W., Miller, W., Myers, E. W., and Lipman, D. J. (1990) *J. Mol. Biol.* **215,** 403–410
15. Berman, H. M., Westbrook, J., Feng, Z., Gilliland, G., Bhat, T. N., Weissig, H., Shindyalor, I. N., and Bourne, P. N. (2000) *Nucleic Acids Res.* **28,** 235–242
16. Frankenberg, N., Erskine, P. T., Cooper, J. B., Shoolingin-Jordan, P. M., Jhan, D., and Heinz, D. W. (1999) *J. Mol. Biol.* **289,** 591–602
17. Frere, F., Schubert, W., Stauffer, F., Frankenberg, N., Neier, R., Jahn, D., and Heinz, D. W. (2002) *J. Mol. Biol.* **320,** 237–247
18. Smith, T. F., and Waterman, M. S. (1981) *J. Mol. Biol.* **147,** 195–197
19. Thompson, J. D., Higgins, D. G., and Gibson, T. J. (1994) *Nucleic Acids Res.* **22,** 4673–4680
20. Holm, L., and Sander, C. (1995) *Trends Biochem. Sci.* **20,** 478–480
21. Foth, B. J., Ralph, S. A., Tonkin, C. J., Struck, N. S., Fraunholz, M., Roos, D. S., Cowman, A. F., and McFadden, G. I. (2003) *Science* **299,** 705–708
22. Jaffe, E. K. (1995) *J. Bioeng. Biomembr.* **27,** 169–179
23. Boese, Q. F., Spano, A. J., Li, J. M., and Timko, M. P. (1991) *J. Biol. Chem.* **266,** 17060–17066
24. Senior, N. M., Brocklehurst, K., Cooper, J. B., Wood, S. P., Erskine, P., Shoolingin-Jordan, P. M., Thomas, P. G., and Warren, M. J. (1996) *Biochem. J.* **320,** 401–412
25. Bevan, D. R., Bodlaender, P., and Shemin, D. (1980) *J. Biol. Chem.* **255,** 2030–2035
26. Frankenberg, N., Heinz, D. W., and Jahn, D. (1999) *Biochemistry* **38,** 13968–13975
27. Jaffe, E. K. (2003) *J. Biol. Inorg. Chem.* **8,** 176–184
28. Erskine, P. T., Senior, N., Awan, S., Lambert, R., Lewis, G., Tickle, I. J., Sarwan, M., Spencer, P., Thomas, P., Warren, M. J., Shoolingin-Jordan, P. M., Wood, S. P., and Cooper, J. B. (1997) *Nat. Struct. Biol.* **12,** 1025–1031
29. Erskine, P. T., Norton, E., Cooper, J. B., Lambert, R., Coker, A., Lewis, G., Spencer, P., Sarwan, M., Wood, S. P., Warren, M. J., and Shoolingin-Jordan, P. M. (1999) *Biochemistry* **38,** 4266–4276
30. Castagnetto, J. M., Hennessy, S. W., Roberts, V. A., Getzoff, E. D., Tainer, J. A., and Pique, M. E. (2002) *Nucleic Acids Res.* **30,** 379–382
31. Chakrabarti, P. (1990) *Protein Eng.* **1,** 49–56
32. Zimmermann, J. L., Amano, T., and Sigalat, C. (1999) *Biochemistry* **46,** 15343–15351
33. Chakrabarti, P. (1990) *Protein Eng.* **1,** 57–63
34. Tschudy, D. P., Hess, R. A., and Frykholm, B. C. (1981) *J. Biol. Chem.* **256,** 9915–9923
35. He, C. Y., Striepen, B., Pletcher, C. H., Murray, J. M., and Roos, D. S. (2001) *J. Biol. Chem.* **276,** 28436–28442
36. Frankenberg, N., Jahn, D., and Jaffe, E. K. (1999) *Biochemistry* **38,** 13976–13982
37. Jaffe, E. K. (2003) *J. Biol. Inorg. Chem.* **8,** 176–184
38. Kohler, S., Delwiche, C. F., Denny, P. W., Tilney, L. G., Webster, P., Wilson, R. J. M., Palmer, D. J., and Roos, D. S. (1997) *Science* **275,** 1485–1489
39. Le Roch, K. G., Zhou, Y., Blair, P. L., Grainger, M., Moch, J. K., Haynes, J. D., Vega, P. D., Holder, A. A., Batalov, S., Carucci, D. J., and Winzeler, E. A. (2003) *Science* **301,** 1503–1508